Environmental Science & Technology

Article

pubs.acs.org/est

Transformation of Pristine and Citrate-Functionalized CeO_2 Nanoparticles in a Laboratory-Scale Activated Sludge Reactor

Lauren E. Barton,[†,‡,§,∥] Melanie Auffan,[§,∥] Marie Bertrand,[∥,⊥] Mohamed Barakat,[∥,⊥] Catherine Santaella,[∥,⊥] Armand Masion,[§,∥] Daniel Borschneck,[§,∥] Luca Olivi,[∇] Nicolas Roche,[#] Mark R. Wiesner,[*,†,‡] and Jean-Yves Bottero[§,∥]

[†]Department of Civil and Environmental Engineering, Duke University, Durham, North Carolina 27708-0287, United States

[‡]Center for the Environmental Implications of Nanotechnology (CEINT), Duke University, Durham, North Carolina 27708-0287 United States

[§]CNRS, Aix-Marseille Université, IRD, Centre Européen de Recherche et Enseignement des Géosciences de l'Environnement (CEREGE), UM34, UMR 7330, 13545 Aix-en-Provence, France

[∥]CNRS, International Consortium for the Environmental Implications of Nanotechnology (iCEINT), 13545 Aix-en-Provence, France

[⊥]CNRS, CEA Cadarache DSV/IBEB/SBVME, Laboratoire d'Écologie Microbienne de la Rhizosphère et d'Environnements Extrêmes (LEMiRE), Aix-Marseille Université, UMR 7265, 13115 Saint-Paul-lès-Durance, France

[#]CNRS, Aix-Marseille Université, M2P2, Traitement des Eaux et des Déchets, UMR 7340, 13545 Aix-en-Provence, France

[∇]Elettra-Sincrotrone, 34149 Basovizza, Trieste, Italy

Supporting Information

ABSTRACT: Engineered nanomaterials (ENMs) are used to enhance the properties of many manufactured products and technologies. Increased use of ENMs will inevitably lead to their release into the environment. An important route of exposure is through the waste stream, where ENMs will enter wastewater treatment plants (WWTPs), undergo transformations, and be discharged with treated effluent or biosolids. To better understand the fate of a common ENM in WWTPs, experiments with laboratory-scale activated sludge reactors and pristine and citrate-functionalized CeO_2 nanoparticles (NPs) were conducted. Greater than 90% of the CeO_2 introduced was observed to associate with biosolids. This association was accompanied by reduction of the Ce(IV) NPs to Ce(III). After 5 weeks in the reactor, 44 ± 4% reduction was observed for the pristine NPs and 31 ± 3% for the citrate-functionalized NPs, illustrating surface functionality dependence. Thermodynamic arguments suggest that the likely Ce(III) phase generated would be Ce_2S_3. This study indicates that the majority of CeO_2 NPs (>90% by mass) entering WWTPs will be associated with the solid phase, and a significant portion will be present as Ce(III). At maximum, 10% of the CeO_2 will remain in the effluent and be discharged as a Ce(IV) phase, governed by cerianite (CeO_2).

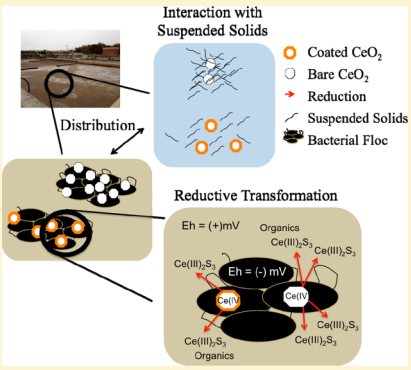

1. INTRODUCTION

The unique properties of engineered nanomaterials (ENMs) are exploited to enhance a variety of technologies and consumer products.[1] The mounting growth of applications of ENMs will inevitably result in their release into the environment.[2,3] One of the primary routes of environmental exposure of many metallic nanoparticles (NPs) is through wastewater treatment plants (WWTPs).[4] To understand the possible fate of ENMs, their distribution and transformations during wastewater treatment must be considered. ENMs may undergo multiple transformations, and the kinetics of these reactions can be altered over time.[5,6] Transformations of metal-containing NPs may include redox reactions, dissolution, adsorption (i.e., physisorption, ion exchange, chemisorption), desorption, precipitation of new phases, and aggregation (homoaggregation with other NPs or heteroaggregation with background particles). Environmental factors that may affect ENM transformations include pH, redox potential, and the quantity and composition of natural organic matter.[6] Many ENM transformations are irreversible and will be the primary determinants of ENM fate, transport, and toxicity.[7] Transformations mediated by microorganisms can alter the core ENM as well as surface functionality, the latter leading to possible changes in surface composition, aggregation state, reactivity, and toxicity potential.[6,8,9]

It has been shown that silver NPs entering WWTPs primarily associate with the biosolids and, regardless of surface

Received: November 6, 2013
Revised: April 4, 2014
Accepted: May 28, 2014
Published: May 28, 2014

 © 2014 American Chemical Society

functionality, undergo oxysulfidation prior to release in effluent and biosolids.[10−13] This sulfidation results in changes in reactivity with respect to dissolution potential, in addition to changes in mobility and bioavailability of the NPs, ultimately impacting their environmental risks.[13−15]

ZnO NPs also undergo critical transformations in wastewater treatment and subsequent sludge composting.[16] Speciation data indicate that ZnO is transformed rapidly into ZnS during wastewater treatment; however, the ZnS is lost during composting, and most of the Zn is associated with phosphorus and iron hydroxides during aerobic composting. It is these final transformation products that will be present in biosolids entering landfills or incinerators or applied to land, while ZnS is anticipated to be the dominant species of Zn in wastewater effluents. As with Ag, these transformations of Zn will greatly impact exposure and hazard potential in the environment.

The current work considers the transformation of another common inorganic ENM that will likely be released to WWTPs, CeO_2. Transformations of two varieties of CeO_2 NPs, pristine and citrate-functionalized, were followed in an aerobic bioreactor simulating wastewater treatment by conventional activated sludge. CeO_2 is an ENM used in a variety of consumer, industrial, and medical applications. It is commonly used in vehicle exhaust systems as a catalytic fuel additive to promote combustion.[17] CeO_2 can further be utilized as a chemical and mechanical polishing agent in the semiconductor industry, a UV light absorber, and a fuel cell electrolyte, and it has also been found to possess antioxidant properties, which could lead to applications in the medical field for cell protection against radiation, oxidative stress, and inflammation.[18] Environmental exposure to CeO_2 NPs is anticipated from several possible pathways. In addition to direct discharge to wastewater, atmospheric releases of CeO_2 have been documented by Park et al. in the form of particulate matter generated from nano-CeO_2-enhanced fuel additives for diesel engines.[19] They observed that the release resulted in slightly increased concentrations of CeO_2 in the soils immediately surrounding roadways in the UK. As in WWTPs, there is the possibility for redox transformation in soils. Further transformation and subsequent exposure to aquatic environments via erosion and runoff are likely. The complex redox chemistry of CeO_2 combined with its small size and associated reactivity are anticipated to affect the fate and transport of CeO_2 NPs.[20]

In addition, previous studies have shown CeO_2 toxicity to microbial communities associated with the reduction of cerium from Ce(IV) to Ce(III).[21,22] Pristine CeO_2 NPs are characterized at neutral pH by a near-neutral net surface charge, which allows for favorable interaction with the negatively charged surface of bacteria. Direct contact between pristine CeO_2 NPs and bacterial membranes is thought to favor Ce reduction and oxidation of the cell membrane.[21,22] Thus, in addition to changing the subsequent toxicity of the CeO_2 NPs, reductive transformation of CeO_2 NPs in the presence of activated sludge bacteria might be anticipated to provoke changes in the microbial community within activated sludge units. However, in the current work we focus uniquely on possible transformations to the CeO_2 NPs that may occur in the presence of aerobic bacteria under highly aerated conditions representative of those present in activated sludge basins.

2. EXPERIMENTAL SECTION

2.1. Materials. The pristine (no specific surface treatment) CeO_2 NPs used in this work were commercially available (Rhodia, France) crystallites of cerianite with diameters of 3−4 nm, as viewed by transmission electron microscopy (TEM; see Supporting Information, Figure S1), where the Ce exists in the 4+ oxidation state. TEM images were obtained using a JEOL 2010F instrument operating at 200 kV. Sample preparation involved placing a droplet of the stock suspension on a carbon-coated copper grid and allowing it to evaporate at room temperature. The average hydrodynamic diameter in the stock suspension as measured by dynamic light scattering (DLS) for pristine CeO_2 was approximately 8 ± 2 nm. The zeta (ζ) potential calculated from electrophoretic mobility measurements (Zetasizer, Malvern, UK) for pristine CeO_2 NPs approached 0 in the stock suspension at environmentally relevant pH values.[23] Citrate-functionalized CeO_2 NPs were provided in a liquid stock by Byk-Gardner GMBH (Geretsried, Germany). They were also made of 3−4 nm crystallites of cerianite with an average hydrodynamic diameter reported by the supplier to be 10 nm. The ζ potential was relatively constant at −45 ± 5 mV over a pH range from 3 to 10 due to the negatively charged citrate coating.[23] Citrate-functionalized CeO_2 NPs are used for UV absorbance applications in floor and furniture wood coatings for long-term protection with high transparency. The differences in surface functionalization and ζ potential between these two variants were hypothesized to affect the colloidal stability of these particles in environmental media, thus impacting the NPs' fate, transport, and affinity for attachment to bacterial surfaces.

Activated sludge was sampled from the aeration basin of an urban WWTP in Aix-en-Provence, France (165,000 inh eq.). The sludge was concentrated to 10 g/L, which was maintained over the 6-week life of the two reactors. Aeration within the 10 L reactor was maintained at 200 L/h, which provided a dissolved oxygen content between 1 and 2.5 mg/L, which is within the 1−3 mg/L range of typical activated sludge operation.[24] Recycle was simulated by pumping 9% of the sludge matrix from the base of the reactor and reintroducing it at the top to maintain homogeneity. The solids' residence time was maintained at 20 days by withdrawing 500 mL of the suspension daily. The sludge was fed with a synthetic substrate, which was composed of 77% sucrose and 23% liquid meat extract (Viandox, Knorr-Unilever, Rueil-Malmaison, France), at a constant mass loading rate equal to 0.25 g COD (Chemical Oxygen Demand) g^{-1} TSS day^{-1} in order to maintain the TS concentration.[25] One gram of sucrose was equivalent to one gram of COD, and one gram of Viandox was equivalent to 0.25 g of COD. Viandox addition was adjusted, as necessary, to decrease the nitrogen input and maintain the filamentous bacterial communities at a minimum level.

A concentration of 100 μg/L of pristine or citrate-functionalized CeO_2 NPs was added to the two separate reactors three times weekly to achieve a final concentration of approximately 1.5 mg/L after 6 weeks. This rate of addition was chosen to mimic CeO_2 maximum concentrations expected in wastewater influent, which was determined on the basis of maximal case scenario estimates of CeO_2 NP production in the amount of 700 tons per year published by Hendren et al.[26] A worst-case scenario (maximum concentration) of 100 μg/L three times weekly was calculated, assuming that approximately half of the CeO_2 NPs produced would be released from products and exposed to wastewaters. The semichronic addition method was employed in an effort to better resemble realistic scenarios of CeO_2 NPs release to the waste stream, which would be continuous.

2.2. Analysis. *Reactor Analysis.* The initial state (after a start-up period of 4−6 weeks but prior to CeO_2 NPs addition) of the reactors was analyzed to confirm that both reactors were compositionally similar prior to amendment with CeO_2 NPs. Sludge was sampled, freeze-dried, and analyzed by powder X-ray diffraction (XRD) and micro-X-ray fluorescence (μXRF) to determine the mineralogical and elemental composition (Supporting Information). The X-ray diffractometer (Panalytical X'Pert Pro MPD) was equipped for Co Kα radiation (1.79 Å) and operated at 40 kV and 40 mA current. A counting time of 400 s per 0.03° step was used for the 2θ range of 10−70°. The X-ray fluorescence microscope (XGT 7000, Horiba Jobin Yvon) was equipped with an X-ray guide tube that produced a finely focused beam with a 100 μm spot size (Rh X-ray tube, 30 kV, 1 mA equipped with an EDX detector).

^{13}C NMR spectroscopy was employed for compositional analysis of bacterially generated extracellular polymeric substances (EPSs) (Supporting Information). EPSs are known to exist in two major phases, freely suspended in solution and more tightly associated with the surface of the bacterial floc. The method for separation of free EPS and bound EPS from the bacteria was detailed by Akkache et al.[25] Following this separation, the two samples from both reactors were freeze-dried for ^{13}C NMR analysis. Solid-state $^{13}C-^{1}H$ cross-polarization magic angle spinning (CP-MAS) NMR analyses were carried out at a frequency of 101.6 MHz on a Bruker AvanceWB 400 MHz spectrometer. Samples were packed into a 4 mm zirconia rotor and spun at 10 kHz in a MAS probe. Cross-polarization was performed with a ramped 1H pulse to circumvent the Hartmann−Hahn mismatches. All spectra were obtained with a 2 ms contact time and 2 s recycling time. To improve the resolution, dipolar decoupling was applied on protons during acquisition. Chemical shifts were referenced to tetramethylsilane.

Finally, the microbial community structure was investigated to ensure that the starting communities in the two reactors matched. One milliliter of the bioreactor sludge was centrifuged at 16110*g* for 15 min. DNA was extracted from the solid phase using the Fast DNA spin kit for soil and an MP Bio FastPrep according to the manufacturer's protocol. Extracted DNA (100 μL) was quantified using a Nanovue spectrophotometer. SSU rRNA gene amplification was performed with barcoded primers for the V1−V3 regions. The 16S universal eubacterial primers 27Fmod (5′-AGRGTTTGATCMTGGCTCAG) and 519R (5′-GTNTTACNGCGGCKGCTG) were used for amplifying the ∼500 bp region of the 16S rRNA genes. The 454 Titanium sequencing run was performed on a 70675 GS PicoTiterPlate by using a Genome Sequencer FLX System (Roche, Nutley, NJ). Sequences were depleted of barcodes and primers, short sequences <200 bp were removed, sequences with ambiguous base calls were removed, and sequences with homopolymer runs exceeding 6 bp were removed. Sequences were then denoised, and chimeras were removed. Operational taxonomic units (OTUs) were defined after removal of singleton sequences, clustering at 3% divergence (97% similarity).[27] OTUs were then taxonomically classified using RPD Classifier (Ribosomal Database Project, http://rdp.cme.msu.edu/classifier/classifier.jsp) and compiled at each taxonomic level into both "counts" and "percentage" files. The R software (http://www.r-project.org) was used to calculate the α-diversity indices (Shannon−Wiener index) and β-diversity index (Bray−Curtis similarity index). Statgraphics Centurion XVI was used to perform statistical analyses.

Distribution of Ce in the Bioreactor. The time-dependent affinity of CeO_2 NPs for the liquid and solid phases of the sludge within the aerobic reactors was monitored by ICP-OES. Weekly sampled sludge was centrifuged at 4000*g* for 15 min to separate the phases. The liquid phase was subsequently acidified with 5% trace metal grade HNO_3, and the solids were oven-dried. In most cases, the concentration of CeO_2 associated with the solid phase was determined by mass balance. However, to confirm mass balance, a few of the solid samples were digested using EPA Method 200.7.[28] Following measurement of Ce in the supernatant (also considered in association with free EPS), Ce was measured in association with bound EPS upon separation.[25] In this study, the more strongly linked EPS, or the "bound" phase of EPS, is more specifically defined as those small molecular weight proteins and substances that are liberated through short sonication of the centrifuged solids resuspended in nanopure water.[25] The measured Ce concentration in each phase was then normalized by the total organic carbon (TOC) in the "free" and "bound" phases, respectively. TOC was measured on a Shimadzu TOC-L analyzer for each phase.

In addition, the colloidal stability of the NPs was assessed in the environmental matrix of WWTP supernatant to observe the interactions between stable stock NP suspensions and the suspended solids in wastewater. The supernatant was separated from activated sludge using gravity settling, mimicking liquid−solid separation in WWTPs. The particle size distribution of the suspended solids in simulated effluent was monitored using a Malvern Mastersizer 3000 particle size analyzer and the refractive index of carbon. Size measurements were conducted at 10 s intervals, and obscuration was maintained in the correct range for optimal measurement. Pristine and functionalized CeO_2 NPs were spiked into the supernatant at different concentrations between 1 and 50 mg/L, and the evolution of the diameter of suspended solids was tracked.

Transformation of CeO_2. Transformations of CeO_2 NPs in wastewater were monitored by following the cerium L_3-edge X-ray absorption near-edge structure (XANES) spectra collected on the X-ray absorption fine structure (XAFS) bending magnet beamline (11.1) at the Elettra-Trieste Synchrotron Light Source (Italy) using a Si(111) monochromator. Samples were collected from each bioreactor after 5 weeks of incubation. The liquid and solid phases were separated via centrifugation at 4000*g* for 15 min, freeze-dried, pressed into 13 mm pellets, and analyzed at room temperature in fluorescence mode. Potential beam damage due to the analysis at room temperature was checked. XANES spectra acquired at 15−20 °C or in a liquid nitrogen cryostat were then compared. No change in the position or shape of the spectra was observed, evidencing the absence of beam damage. In addition to measurements on the bioreactor samples, Ce(IV) and Ce(III) references powders were diluted in PVP, pressed into 13 mm pellets, and measured in transmission mode. The Ce(IV) references included the NPs, pristine and citrate-functionalized, along with Ce(III) carbonate, Ce(III) sulfate, and Ce(III) oxalate. The spectra presented are the sums of 3−5 scans. The energy was calibrated using a macroscopic CeO_2 reference compound. XANES spectra were pre-edge subtracted and normalized using IFEFFIT software.[29] Least-squares optimization of linear combination fitting (LCF) was also performed using IFEFFIT. The precision of LCF is estimated to be ±10%.

Kinetics of Transformation. For assessment of the kinetics of the CeO_2 transformations, a spike experiment was performed

with 0.4 mg Ce/30 mg sludge to optimize the $\Delta\mu$ during XANES analysis at the Ce L_3-edge analysis. Wastewater sludge not yet contaminated with CeO_2 was sampled from the bioreactor and mixed with either pristine or citrate-functionalized NPs for multiple time periods between 1 h and 1 day. Samples were prepared in the same manner. The samples were then measured in transmission mode, and LCF was completed for data analysis with the same reference compounds.

3. RESULTS AND DISCUSSION

3.1. Bioreactor Initial Analysis. Initial characterization of the sludge from the two reactors by XRD and μXRF indicated the presence of three dominant mineral phases—quartz, halite, and calcite—and a number of dominant elements, all listed in Table S1. The diffractograms and elemental composition for the two reactors were in good agreement, suggesting similar mineral and chemical composition of the sludge prior to spiking with CeO_2 NPs.

The ^{13}C NMR spectra (Figure S2) for the bound and free phases of EPS were observed to be similar. The majority of the EPS molecules consisted of proteins and polysaccharides (45−65 ppm and >110 ppm, as shown in Figure 2 in the next section), which is in agreement with previous studies.[30−32] At the initial time point, the bound EPS was compositionally different from the free EPS, meaning the types of proteins and carbohydrates varied depending on the phase of EPS analyzed. However, the two phases, bound and free EPS, from reactor 1 (prior to addition of pristine CeO_2 NPs) matched the same respective fractions in reactor 2 (prior to addition of citrate-functionalized CeO_2 NPs). Major peaks corresponding to carbohydrates and proteins are detailed in Table S2. The spectra measured for the EPS generated by the sampled wastewater sludge in these reactors suggested strong similarities in the different regions with spectra from other isolated EPS fractions.[33]

Finally, the similarity of the two reactors before ENM addition was assessed in terms of microbial community composition by 16S rRNA gene pyrosequencing. Table S3 shows the different indices characterizing the α-diversity (Richness and Shannon−Wiener indices) and β-diversity (Bray−Curtis dissimilarity) of samples. Minor variations in the α-diversity of microbial communities present in each sludge were observed. Bray−Curtis dissimilarity between two samples varies in the 0−1 range, where two communities that share no OTUs have a maximum Bray−Curtis dissimilarity of 1, while 0 means the samples are exactly the same. A dissimilarity of 0.32 thus indicated good agreement between the compositions in the two reactors.

As shown in Figure 1, the microbial community structures on the phylum level were alike in terms of dominant phyla and in the content of each phylum.[34] Based on the sign and signed rank test, comparison of microbial populations in the two reactors (paired samples) at the phylum level showed no significant differences between the two data samples ($p > 0.05$). The most predominant phyla, *Proteobacteria*, *Bacteroidetes*, and *Actinobacteria*, have been previously identified as major phyla in activated sludges.[34] In summary, these data show that the elemental, mineralogical, EPS, and microbial compositions are similar in the two bioreactors prior to addition of NPs (t_0).

3.2. Ce Distribution. Distribution experiments indicated a high affinity of the CeO_2 NPs for the solids relative to the liquid phase regardless of surface treatment, with >90% of the particles retained in the solid matrix. As can be seen in Figure 2A, after 6 weeks in the bioreactors and addition of 1.5 mg/L NPs, ∼23 μg/L of pristine CeO_2 remained in the effluent, relative to ∼27 μg/L of the functionalized NPs. Other inorganic NPs, including Ag and TiO_2, have been shown to behave similarly, with strong affinities for the solids.[35,36] It has been reported that NPs in complex matrices like sludge will interact with a variety of surface functional groups like acids and hydroxyls, which can improve the affinity for the solid phase, leading to high removal.[14] Figure 2B shows the concentration of NPs associated with the solid phase relative to the concentration added to the experiment. These results confirm that the majority (∼90%) of the CeO_2 NPs interact with the solids. Similar findings were reported where CeO_2 effluent concentrations ranged from 6% to 11% of the total introduced to wastewater.[20,37]

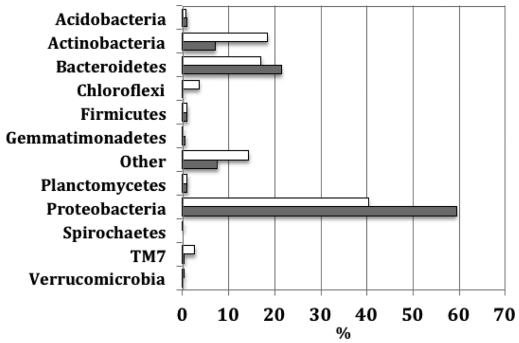

Figure 1. Bacterial community structures in the two bioreactors prior to addition of pristine CeO_2 (reactor 1, white bars) or citrate-functionalized CeO_2 (reactor 2, dark bars) NPs. The abundance is presented as % of the total effective bacterial sequences using RDP Classifier at 97% similarity.

In addition, to investigate colloidal stability imparted by surface functionalization as a function of NP concentration, the effective size of suspended solids in wastewater effluent was analyzed before and after addition of NPs. It was observed that citrate-functionalized particles did not alter the size distribution of effluent-suspended material, which remained constant with a dv_{50}, or median diameter, of 50 μm ± 1%. However, upon addition of the pristine CeO_2 NPs at or greater than 10 mg/L, the hydrodynamic diameter was observed to rapidly increase from 50 μm ± 1% to 130 μm ± 1%. This suggested that the pristine NPs act as a coagulant at higher concentrations and cause suspended solids to aggregate. The increased colloidal stability of the citrate-functionalized NPs in the supernatant explains decreased removal to the solids with concentrations in excess of 10 mg/L.

The Ce associated with the free and bound EPS phases was also analyzed. It was observed that a higher amount of the functionalized CeO_2 NPs associated with both fractions of EPS (Figure 3). It is important to note that the concentration of Ce measured in the EPS did not exceed 15% of the added amount, meaning that the highest portion of the CeO_2 added remained well associated with the intact solids. These results do suggest, though, that the functionalized CeO_2 may be associated to a greater extent with the EPSs that are more loosely arranged in the matrix and therefore liberated, while the pristine CeO_2 may have a higher affinity for the remaining solids composed mostly of bacterial flocs.

3.3. Transformations of CeO_2 NPs in Activated Sludge Bioreactors. The speciation of Ce within the solid phase of each bioreactor after 5 weeks was analyzed using XANES to

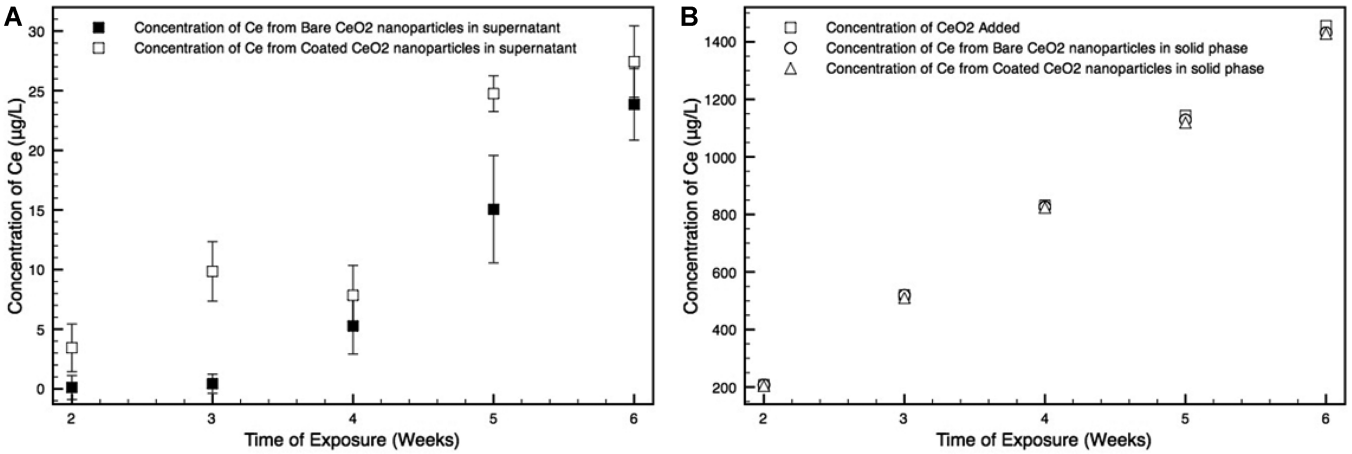

Figure 2. (A) Supernatant-phase Ce concentration (μg/L) over the lifetime of the reactors (~5 weeks). (B) Solid-phase Ce concentration (μg/L) relative to the added concentration.

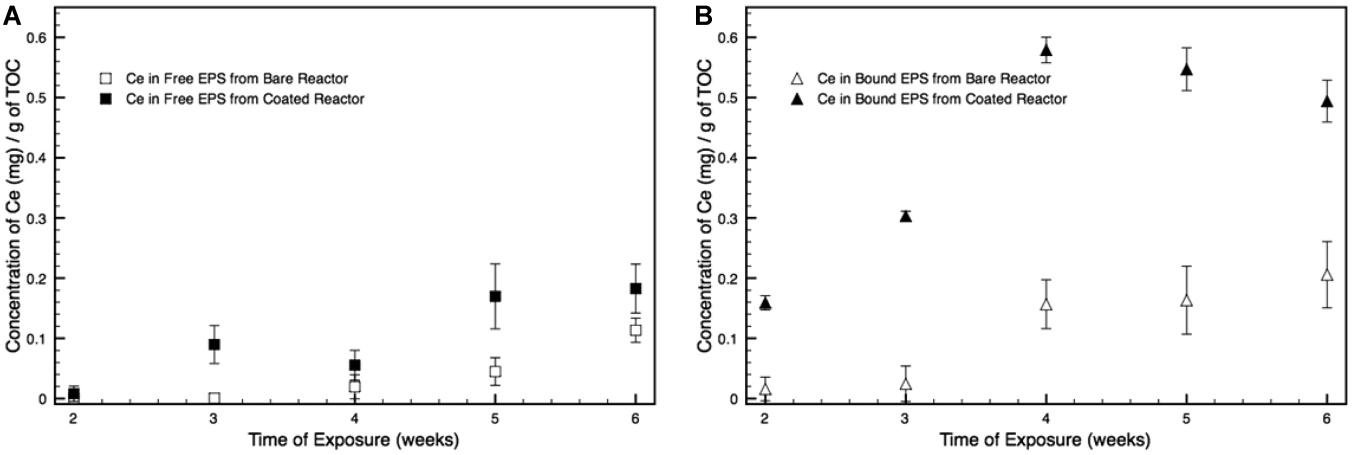

Figure 3. Concentration of Ce from pristine and functionalized CeO_2 amendments associated with (A) the bound fraction and (B) the free fraction of EPS. The data are normalized by the mass of total organic carbon.

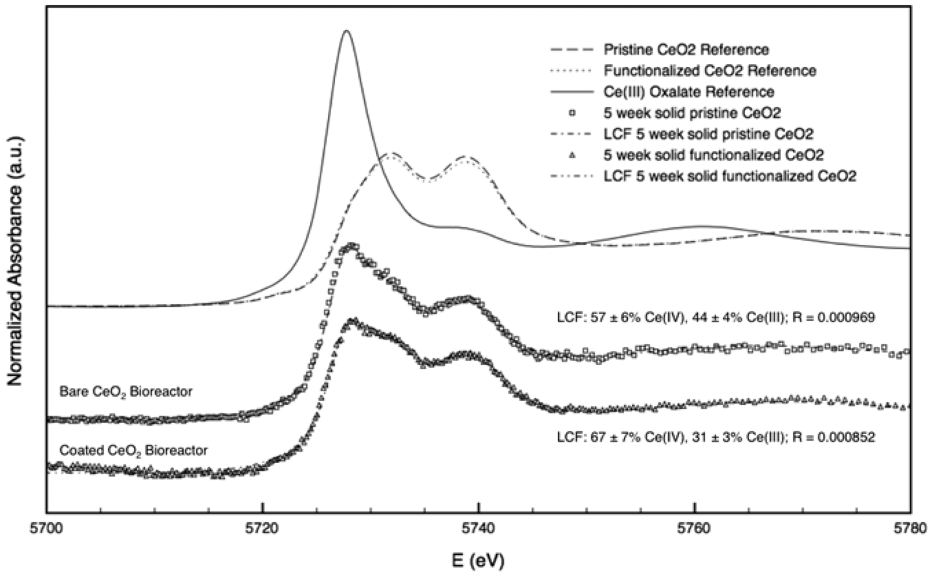

Figure 4. Experimental XANES spectra at the Ce L_3-edge of the Ce present after 5 weeks in the bioreactors contaminated with pristine and citrate-functionalized CeO_2 NPs. XANES spectra of the initial pristine and functionalized NPs as well as the Ce(III) oxalate are provided for reference. The fitted spectra and the results of the LCF are given. R is the fit residue. LCF energy ranges from −6.4 to 18.8 eV around the edge.

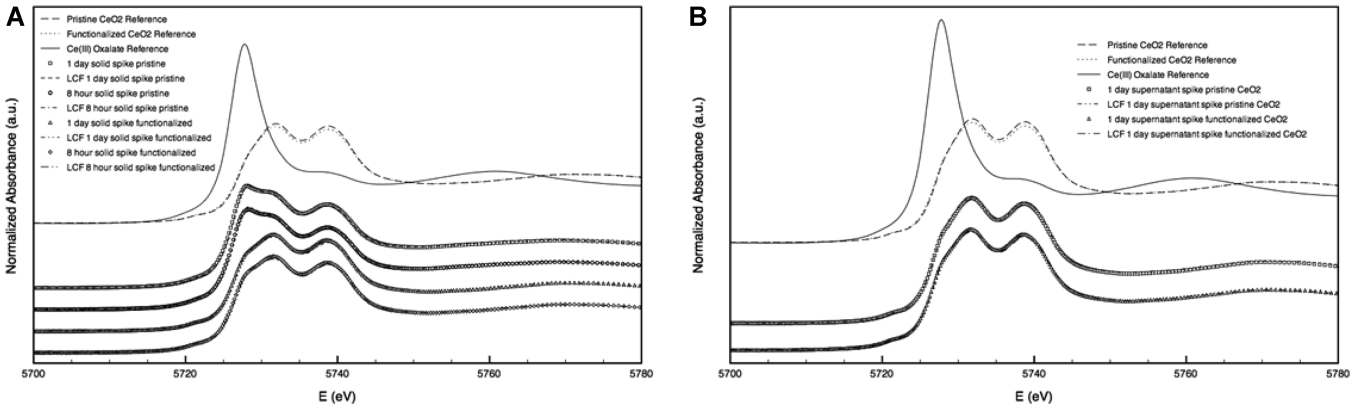

Figure 5. (A) XANES spectra obtained from the solids of a spike experiment with pristine and functionalized CeO_2 NPs and activated sludge where the particles and sludge were mixed for 8 h and 1 day and the Ce XANES spectra were subsequently probed. (B) XANES spectra from the supernatant spike experiment following 1 day of mixing with activated sludge.

determine transformations (Figure 4). The difference in XANES spectra for Ce(IV) versus Ce(III) is easily distinguishable, as Ce(IV) has two absorption peaks at 5733 and 5740 eV, while Ce(III) has one absorption peak at 5729 eV. LCF of the XANES spectra of the initial NP and Ce(III) references (Ce(III) carbonate, oxalate, and sulfate) was used to estimate the percentage of Ce(IV) and Ce(III) in our experimental spectra. The most appropriate Ce(III) reference was determined to be Ce(III) oxalate, which generated the lowest *R* factors.

XANES analysis of the Ce in the bioreactors indicated reduction of the Ce(IV) NPs to a Ce(III) phase. Comparing the two bioreactors, the pristine CeO_2 was reduced more rapidly (44 ± 4% of Ce(III)) relative to the citrate-functionalized CeO_2 (31 ± 3% of Ce(III)) after a period of 5 weeks (Figure 4). The limited rate of reduction of functionalized CeO_2 was likely due to differences in affinity for the bacterial surface, which this work (see Figure 5B in the next section) and another study indicate are necessary for reduction.[22] The citrate functionalization, when present, likely acted as a barrier against interaction with the bacterial surface, limiting the rate of reduction. Previous research indicates that NP aging results in degradation of the citrate coating over time, possibly by changes in chemical equilibrium or bacterial presence.[23] In this study, a chronic input of citrate-functionalized NPs over the life of the reactor would impact the overall rate of reduction, as there would be gradients in citrate degradation.

In this experiment, the reduction occurred in an aerobic or oxidizing system. Therefore, CeO_2 NPs must come into contact with microreducing zones generated by bacterial sludge flocs for Ce reduction to occur. Within microbial flocs, these reducing environments occur as the result of microbial metabolism that depletes the oxygen present, allowing for reduction mechanisms to take place.[38] Thill and Zeyons and co-workers observed such a reduction of CeO_2 NPs to Ce(III) in contact with the membranes of pristine cultures of Gram-negative *E. coli* and *Synechocystis* bacteria.[21,22]

3.4. Kinetics of CeO_2 NPs Transformation. The kinetics of the Ce(IV) reduction were more closely analyzed by XANES following a spike addition of CeO_2 NPs at a higher concentration (0.4 mg Ce/30 mg sludge) added in batch and mixed with sludge for 1 h, 8 h, and 1 day. It is important to note that, when comparing with bioreactor results, changing the NP-to-bacterial surface ratio will impact the rate of transformation; however, it was important to observe the transformation and changes in the rate over time. Figure 5A illustrates the increased reduction of Ce(IV) to Ce(III) as a function of mixing time for pristine and functionalized CeO_2 NPs in contact with the solid phase of activated sludge. Within the first hour, significant reduction (27 ± 3% of Ce(III)) was observed for pristine CeO_2. With mixing times between 1 h and 1 day, the reduction of the pristine CeO_2 did not significantly increase. Comparing the pristine to the citrate-functionalized NPs, the results suggested slowed transformation kinetics, with only about half as much reduction (12 ± 1% of Ce(III)) measured at 8 h and 1 day for the citrate-functionalized CeO_2. Consequently, at 8 h (typical solids residence time in an activated sludge reactor), the functionalized CeO_2 is anticipated to be more chemically stable than the pristine CeO_2 (Figure 5 and Table 1). It has been shown that direct contact with the bacterial membrane is necessary for the reduction to occur and that organics on the surface of microorganisms could limit this reduction by either forming a protective barrier or reducing the affinity for interaction.[22] It can thus be concluded, in agreement with

Table 1. Summary of LCF Results (±10%) of the XANES Spectra in Figure 5 for CeO_2 in the Solid and Liquid Phases of the Spike Experiments with Pristine and Citrate-Functionalized CeO_2 as a Function of Mixing Time[a]

sample	mixing time	% Ce(IV)	% Ce(III)	*R* factor
		Solid Phase		
pristine	1 h	73	27	0.000 270
	8 h	67	33	0.000 281
	1 day	68	33	0.000 317
functionalized	8 h	89	11	0.000 249
	1 day	89	12	0.000 139
		Liquid Phase		
pristine	1 h	>90	<10	0.000 123
	8 h	>90	<10	0.000 106
	1 day	>90	<10	0.000 067
functionalized	8 h	>90	<10	0.000 268
	1 day	>90	<10	0.000 149

[a]Fits were generated with reference spectra for the added nanoparticles, either pristine or citrate-functionalized, and Ce(III) oxalate.

bioreactor results, that the citrate treatment may reduce direct nanoparticle–bacteria contacts and therefore reduce the rate of reduction of the citrate CeO_2 NPs. The transformations of CeO_2 NPs were also investigated in the liquid phase of the spiked samples (Figure 5, Table 1). Both pristine and functionalized CeO_2 NPs were present in the Ce(IV) phase after 8 h and 1 d in contact with the liquid phase at >90% of the total. It is possible either that those NPs were never reduced or that reoxidation from Ce(III) to Ce(IV) occurred in the oxidizing supernatant. The absence of a Ce(III) phase in the supernatant of the experiment suggests that the solids or bacteria in wastewater are necessary to stimulate reduction of CeO_2 NPs.

3.5. Transformation Products of CeO_2 Reduction in a WWTP. Upon reduction by bacteria in the activated sludge, the Ce(III) is most likely complexed in the solid phase, given the large concentrations of ligands available. If the Ce(III) distributes back to the supernatant, then reoxidation occurs because Ce(III) is not observed in the supernatant, and oxidation is favorable due to the aerobic environment. Typically, EXAFS spectra provide information on the metal binding environment to determine the Ce(III) complex formed; however, interference in the EXAFS region renders this technique unsuitable for Ce. As such, the formation of a Ce(III) complex can be hypothesized on the basis of thermodynamics. The argument for the Ce(III) complexes formed in this system required the investigation of the solid-phase speciation and mineral activity of Ce minerals in wastewater sludge provided in Essington and Mattigod (1985).[39] These authors used mineral activity ratios to analyze the stability of Ce minerals in oxidizing and reducing sludge environments. Their results indicated that, in the oxidizing environment of sewage sludge where the concentration of sulfur is high, $Ce_2(SO_4)_3{\cdot}8H_2O$ would control Ce^{3+} activity. With increasingly oxidizing conditions, cerianite (CeO_2) would be expected to control Ce^{3+} speciation. In addition, the authors found that, under reducing conditions, similar to what is observed in anaerobic digesters, Ce_2S_3 would be the stable solid phase. This would suggest that CeO_2 NPs that undergo reduction in activated sludge result in the formation of $Ce_2(SO_4)_3{\cdot}8H_2O$ that is later transformed to Ce_2S_3 in anaerobic digestion. Another possible metastable phase of cerium is monazite ($CePO_4$), which has been observed in soil environments.[17] This could suggest that further transformation of reduced Ce_2S_3 upon removal from the anaerobic digester to aerobic compositing prior to recycling or disposal of biosolids would be possible.

The results of this work suggest that a significant portion of nanoparticulate (~10 nm) CeO_2 released to WWTPs would associate with the solids where reduction would occur in the activated sludge tank. The presence of an organic coating was observed to slow the kinetics of this reduction. The remaining (<10%) CeO_2 NPs in the liquid phase would be discharged in effluent as CeO_2, which is the mineral phase that governs Ce^{4+} speciation in aerobic environments. These results are of critical importance for predicting concentrations of CeO_2 in the environment following release to the waste stream and indicate that Ce(III) complexes could be of importance to analyze further.

■ ASSOCIATED CONTENT

Supporting Information

Additional figures and tables showing TEM, μXRD, XRD, and NMR of the initial state of the bioreactors. This material is available free of charge via the Internet at http://pubs.acs.org.

■ AUTHOR INFORMATION

Corresponding Author

*Phone: (919) 660-5292; fax: (919) 660-5219; e mail: wiesner@duke.edu.

Notes

Any opinions, findings, conclusions, or recommendations expressed in this material are those of the author(s) and do not necessarily reflect the views of the NSF, EPA, or ANR. This work has not been subjected to EPA review and no official endorsement should be inferred.

The authors declare no competing financial interest.

■ ACKNOWLEDGMENTS

This material is based upon work supported by the NSF and the EPA under NSF Cooperative Agreement EF-0830093, Center for the Environmental Implications of NanoTechnology (CEINT), Transatlantic Initiative for Nanotechnology and the Environment (TINE) supported by the UK Natural Environment (NE/H013679/1; NE/H01375X/1), the French Agence Nationale de la Recherche (ANR P2N 2010, MESONNET project), and the Labex SERENADE (11-LABX-0064). The authors gratefully acknowledge the CNRS for funding the iCEINT International Consortium for the Environmental Implications of Nanotechnology (GDRi iCEINT). Additional financial support was provided by the Research Federation FR-ECCOREV (Project SLUDGE) and the Chateaubriand fellowship from the Embassy of France in the United States. The authors thank the ELETTRA synchrotron in Trieste, Italy, for providing synchrotron beam time and XAFS 11.1 local contacts for their help during the experiment.

■ REFERENCES

(1) Maynard, A. D. Nanotechnology: Assessing the risks. *Nano Today* **2006**, *1* (2), 22–33.

(2) Gottschalk, F.; Nowack, B. The release of engineered nanomaterials to the environment. *J. Environ. Monit.* **2011**, *13* (5), 1145–1155.

(3) Wiesner, M. R.; Lowry, G. V.; Jones, K. L.; Hochella, M. F.; Di Giulio, R. T.; Casman, E.; Bernhardt, E. S. Decreasing uncertainties in assessing environmental exposure, risk, and ecological implications of nanomaterials. *Environ. Sci. Technol.* **2009**, *43* (17), 7458–6462.

(4) Blaser, S. A.; Scheringer, M.; MacLeod, M.; Hungerbuhler, K. Estimation of cumulative aquatic exposure and risk due to silver: Contribution of nano-functionalized plastics and textiles. *Sci. Total Environ.* **2008**, *390* (2–3), 396–409.

(5) Christian, P.; Von der Kammer, F.; Baalousha, M.; Hofmann, T. Nanoparticles: structure, properties, preparation, and behavior in environmental media. *Ecotoxicology* **2008**, *17* (5), 326–343.

(6) Lowry, G. V.; Gregory, K. B.; Apte, S. C.; Lead, J. R. 2012. Transformations of nanomaterials in the environment. *Environ. Sci. Technol.* **2012**, *46* (13), 6893–6899.

(7) Auffan, M.; Rose, J.; Bottero, J.-Y.; Lowry, G. V.; Jolivet, J. P.; Wiesner, M. R. Towards a definition of inorganic nanoparticles from an environmental, health and safety perspective. *Nat. Nanotechnol.* **2009**, *4* (10), 634–641.

(8) Bottero, J.-Y.; Wiesner, M. R. Considerations in evaluating the physicochemical properties and transformations of inorganic nanoparticles in water. *Nanomedicine* **2010**, *5* (6), 1009–1014.

(9) Auffan, M.; Bottero, J.-Y.; Chaneac, C.; Rose, J. 2010. Inorganic manufactured nanoparticles: how their physicochemical properties influence their biological effects in aqueous environments. *Nanomedicine* **2010**, *5* (6), 999−1007.

(10) Kaegi, R.; Voegelin, A.; Sinnet, B.; Zuleeg, S.; Hagendorfer, H.; Burkhardt, M.; Siegrist, H. Behavior of metallic silver nanoparticles in a pilot wastewater treatment plant. *Environ. Sci. Technol.* **2011**, *45* (9), 3902−3908.

(11) Liu, G.; Wang, D.; Wang, J.; Mendoza, C. Effect of ZnO particles on activated sludge: role of particle dissolution. *Sci. Total Environ.* **2011**, *409* (14), 2852−2857.

(12) Doolette, C. L.; McLaughlin, M. J.; Kirby, J. K.; Batstone, D. J.; Harris, H. H.; Ge, H.; Cornelis, G. Transformation of PVP coated silver nanoparticles in simulated wastewater treatment processes and the effect on microbial communities. *Chem. Cent. J.* **2013**, *7* (46), 2−18.

(13) Ma, R.; Levard, C.; Marinakos, S.; Chen, Y.; Liu, J.; Brown, G. E., Jr.; Lowry, G. V. Size controlled dissolution of organic-coated silver nanoparticles. *Environ. Sci. Technol.* **2012**, *46*, 752−759.

(14) Levard, C.; Reinsch, B. C.; Michel, F. M.; Oumahi, C.; Lowry, G. V.; Brown, G. E. 2011. Sulfidation processes of PVP-coated silver nanoparticles in aqueous solution: Impact on dissolution rate. *Environ. Sci. Technol.* **2011**, *45*, 5260−5266.

(15) Levard, C.; Hotze, E. M.; Lowry, G. V.; Brown, G. E. Environmental transformations of silver nanoparticles: Impact on stability and toxicity. *Environ. Sci. Technol.* **2012**, *46*, 6900−6914.

(16) Lombi, E.; Donner, E.; Tavakkoli, E.; Turney, T. W.; Naidu, R.; Miller, B. W.; Scheckel, K. G. Fate of zinc oxide nanoparticles during anaerobic digestion of wastewater and post-treatment processing of sewage sludge. *Environ. Sci. Technol.* **2012**, *46* (16), 9089−9096.

(17) Cornelis, G.; Kirby, J. K.; Beak, D.; Chittleborough, D.; McLaughlin, M. J. A method for determination of retention of silver and cerium oxide manufactured nanoparticles in soils. *Environ. Chem.* **2010**, *7*, 298−308.

(18) Pelletier, D. A.; Suresh, A. K.; Holton, G. A.; McKeown, C. K.; Wang, W.; Gu, B.; Mortensen, N. P.; Allison, D. P.; Joy, D. C.; Allison, M. R.; Brown, S. D.; Phelps, T. J.; Doktycz, M. J. Effects of engineering cerium oxide nanoparticles on bacterial growth and viability. *Appl. Environ. Microbiol.* **2010**, *76* (24), 7981−7989.

(19) Park, B.; Donaldson, K.; Duffin, R.; Tran, L.; Kelly, F.; Mudway, I.; Morin, J. P.; Guest, R.; Jenkinson, P.; Samaras, Z.; Giannouli, M.; Kouridis, H.; Martin, P. Hazard and risk assessment of a nanoparticulate cerium-oxide based diesel fuel additive—a case study. *Inhalation Toxicol.* **2008**, *20*, 547−566.

(20) Gomez-Rivera, F.; Field, J. A.; Brown, D.; Sierra-Alvarez, R. Fate of cerium dioxide (CeO_2) nanoparticles in municipal wastewater during activated sludge treatment. *Bioresour. Technol.* **2012**, *108*, 300−304.

(21) Thill, A.; Zeyons, O.; Spalla, O.; Chauvat, F.; Rose, J.; Auffan, M.; Flank, A. M. Cytotoxicity of CeO_2 nanoparticles for Escherichia coli. Physico-chemical insight of the cytotoxicity mechanism. *Environ. Sci. Technol.* **2006**, *40* (19), 6151−6156.

(22) Zeyons, O.; Thill, A.; Chauvat, F.; Menguy, N.; Cassier-Chauvat, C.; Orear, C.; Daraspe, J.; Auffan, M.; Rose, J.; Spalla, O. Direct and indirect CeO_2 nanoparticles toxicity for Escherichia coli and Synechocystis. *Nanotoxicology* **2009**, *3* (4), 284−295.

(23) Auffan, M.; Masion, A.; Labille, J.; Diot, M.-A.; Liu, W.; Olivi, L.; Proux, O.; Ziarelli, F.; Chaurand, P.; Geantet, C.; Bottero, J.-Y.; Rose, J. Long-term aging of a CeO2 based nanocomposite used for wood protection. *Environ. Pollut.* **2014**, *188*, 1−7.

(24) Tchobanoglous, G., Burton, F. L., Stensel, H. D., Eds. *Wastewater engineering: treatment, disposal and reuse, Metcalf & Eddy, Inc.*, 4th ed.; McGraw-Hill, Inc.: New York, 2003.

(25) Akkache, S.; Seyssieq, I.; Roche, N. Effect of exo polysaccharide concentration in the rheological properties and settling ability of activated sludge. *Environ. Technol.* **2013**, 1−9.

(26) Hendren, C. O.; Mesnard, X.; Droge, J.; Wiesner, M. R. Estimating production data for five engineered nanomaterials as a basis for exposure assessment. *Environ. Sci. Technol.* **2011**, *45* (7), 2562−2569.

(27) Dowd, S. E.; Hanson, J. D.; Rees, E.; Wolcott, R. D.; Zischau, A. M.; Sun, Y.; White, J.; Smith, D. M.; Kennedy, J.; Jones, C. E. Survey of fungi and yeast in polymicrobial infections in chronic wounds. *J. Wound Care* **2011**, *20* (1), 40−47.

(28) Martin, T. D., Brockhoff, C. A., Creed, J. T., and EMMC Methods Work Group. Method 200.7, Determination of metals and trace elements in water and wastes by inductively coupled plasma−atomic emission spectroscopy, Revision 4.4, EMMC Version; U.S. Environmental Protection Agency: Cincinnati, OH, 1994.

(29) Ravel, B.; Newville, M. ATHENA, ARTEMIS, HEPHAESTUS: data analysis for X-ray absorption spectroscopy using IFEFFIT. *J. Synchrotron Radiat.* **2005**, *12*, 537−541.

(30) Jorand, F.; Zartarian, F.; Thomas, F.; Block, J. C.; Bottero, J.-Y.; Villemin, G.; Urbain, V.; Manem, J. Chemical and structural (2D) linkage between bacteria within activated sludge flocs. *Water Res.* **1995**, *29* (7), 1639−1647.

(31) Cadoret, A.; Conrad, A.; Block, J.-C. Availability of low and high molecular weight substrates to extracellular enzymes in whole and dispersed activated sludges. *Enzyme Microb. Technol.* **2002**, *31* (1−2), 179−186.

(32) Martin-Cereceda, M.; Jorand, F.; Guinea, A.; Block, J.-C. Characterization of extracellular polymeric substances in rotating biological contactors and activated sludge flocs. *Environ. Technol.* **2001**, *22* (8), 951−959.

(33) Metzger, U.; Lankes, U.; Fischpera, K.; Frimmel, F. H. The concentration of polysaccharides and proteins in EPS of Pseudomonas putida and Aureobasidum pullulans are revealed by ^{13}C CPMAS NMR spectroscopy. *Appl. Microbiol. Biotechnol.* **2009**, *85*, 197−206.

(34) Hu, M.; Wang, X.; Wen, X.; Xia, Y. Microbial community structures in different wastewater treatment plants as revealed by 454-pyrosequencing analysis. *Bioresour. Technol.* **2012**, *117*, 72−79.

(35) Kiser, M. A.; Ryu, H.; Jang, H.; Hristovski, K.; Westerhoff, P. Biosorption of nanoparticles to heterotrophic wastewater biomass. *Water Res.* **2010**, *44* (14), 4105−4114.

(36) Hendren, C. O.; Badireddy, A. R.; Casman, E.; Wiesner, M. R. Modeling nanomaterial fate in wastewater treatment: Monte Carlo simulation of silver nanoparticles (nano-Ag). *Sci. Total Environ.* **2013**, *449*, 418−425.

(37) Limbach, L. K.; Bereiter, R.; Muller, E.; Krebs, R.; Galli, R.; Stark, W. J. Removal of oxide nanoparticles in a model wastewater treatment pant: Influence of agglomeration and surfactants on clearing efficiency. *Environ. Sci. Technol.* **2008**, *42* (15), 5828−5833.

(38) Li, B.; Bishop, P. L. Oxidation-reduction potential changes in aeration tanks and microprofiles of activated sludge floc in medium- and low-strength wastewaters. *Water Environ. Res.* **2004**, *76* (5), 394−403.

(39) Essington, M. E.; Mattigod, S. V. Lanthanide solid phase speciation. *Soil Sci. Soc. Am. J.* **1985**, *49* (3), 1387−1393.